

# Effect of plasma treatment on the microstructure and electrical properties of MIM capacitors with PECVD silicon oxide and silicon nitride

Chia-Cheng Ho · Bi-Shiou Chiou

Received: 21 November 2005 / Accepted: 15 March 2006 / Published online: 30 December 2006  
© Springer Science+Business Media, LLC 2006

**Abstract** Metal–insulator–metal (MIM) capacitors with plasma enhanced chemical vapor deposited (PECVD) nitride exhibit trap-induced dispersive behavior and electrical hysteresis, which lead to degradation in capacitor linearity at low frequencies. The dominant defect was suggested to be silicon dangling bonds originated from nitrogen deficiency. Previous methods to eliminate the dispersive behavior and electrical hysteresis include use of oxide–nitride–oxide (ONO) stacks and/or plasma pre-treatment of silicon substrate before nitride deposition [Van Huylbroeck S, Decoutere S, Venegas R, Jenei S, Winderickx G (2002) *IEEE Electron Device Lett* 23:191; Lau WS (1990) *Jpn J Appl Phys* 29:L690]. In this study, the plasma post-treatment method was employed; MIM capacitors with PECVD oxide and nitride were treated with  $N_2O$  and  $SiH_4/NH_3$  plasma, respectively, after deposition of the dielectric layer. No apparent change in film microstructure is observed after plasma treatment. Plasma post-treatment is effective in eliminating the electrical hysteresis shift of the nitride capacitors. Fourier transform infrared (FTIR) absorption spectra suggest an increase of the Si–H bond after  $SiH_4/NH_3$  plasma bombardment of the nitride films. Auger depth profiling indicates a slight increase of nitrogen to silicon ratio after plasma treatment. The increase of

the Si–H bonds as well as the raise of nitrogen to silicon ratio are two possible causes for the elimination of the hysteresis shift of the plasma-treated nitride capacitors. The time dependent dielectric breakdown testing indicates a decrease in both the leakage current and the lifetime of the MIM capacitors treated with plasma. Possible dielectric degradation mechanism is explored.

## Introduction

Integration of precision metal–insulator–metal (MIM) capacitors into high performance technologies has been a key building block for mixed-signal IC applications. Plasma enhanced chemical vapor deposition (PECVD) has the advantage of depositing insulators in a clean processing vicinity at very low temperatures. The low temperature processing eliminates the segregation or redistribution of the dopants commonly occurred in conventional high temperature processes. However, the dielectric to substrate interface properties and the film qualities deteriorate from want of high temperature annealing. Plasma treatment has been used to improve the interfacial properties between the dielectric and the substrate. Chang et al. reported that fluorinated oxides fabricated with PECVD exhibited low leakage current, high breakdown field, and good reliability when subjected to  $CF_4$  plasma treatment [1, 2]. Lim et al. [3] demonstrated that the mobility of a hydrogenated amorphous silicon thin film transistor (a-Si:H TFT) was improved by plasma treatment on the surface of silicon nitride ( $SiN_x$ ) before a-Si:H

C.-C. Ho · B.-S. Chiou  
Department of Electronics Engineering and Institute of Electronics, National Chiao Tung University, Hsinchu, Taiwan, P. R. China

B.-S. Chiou (✉)  
Innovative Packaging Research Center, National Chiao Tung University, Hsinchu, Taiwan, P. R. China  
e-mail: bschiou@mail.nctu.edu.tw

deposition. They attributed the mobility improvement to the decrease of the surface roughness and the rearrangement of the surface atoms of  $\text{SiN}_x$  films. Our previous work reveals that the effect of plasma treatment on hydrogen silesquioxane (HSQ) dielectric films was multiple. The plasma bombardment broke the Si–H bonds of HSQ film and led to the formation of dangling bonds that absorbed water easily. However, the simultaneous annealing and bond rearrangement during plasma bombardment provided a denser film surface that prevented further degradation of HSQ films when more plasma was applied [4].

Metal–insulator–metal (MIM) and metal–nitride–semiconductor (MNS) capacitors with PECVD nitride exhibit trap-induced dispersive behavior and electrical hysteresis, which lead to degradation in capacitor linearity at low frequencies, limiting the accuracy in precision analog circuits [5, 6]. The dominant defect responsible for charge trapping in silicon nitride was suggested to be silicon dangling bonds, which originate from a deficiency in nitrogen. Various methods, such as: use of a PECVD oxide–nitride–oxide (ONO) stacks and/or appropriate  $\text{SiH}_4/\text{NH}_3$  plasma pre-treatment of silicon substrate before the nitride deposition to make the nitrogen to silicon ratio higher at the interfacial region have been employed to eliminate the dispersive behavior and electrical hysteresis [5, 6]. However, very few work reported on the effect of the plasma post-treatment on the electrical behaviors of the dielectric films.

In this study, MIM capacitors with PECVD oxide and nitride were treated with  $\text{N}_2\text{O}$  and  $\text{SiH}_4/\text{NH}_3$  plasma, respectively, after deposition of the dielectric layer. The effects of plasma post-treatment on the microstructure, the electrical behaviors, and the reliability of the dielectric thin films are investigated.

## Experimental procedures

Four-inch diameter p-type (100) Si wafers with nominal resistivity of 1–10  $\Omega\text{-cm}$  were used as substrate. After standard RCA cleaning, a 100 nm  $\text{SiO}_2$  film was grown on the Si substrate. A 100 nm Al films were deposited by thermal evaporation coater onto the  $\text{SiO}_2/\text{Si}$  substrate to serve as the bottom electrode. Two dielectrics,  $\text{SiO}_2$  and  $\text{SiN}_x$ , were prepared in this study. The amorphous  $\text{SiO}_2$  films, deposited by the decomposition of tetraethyl orthosilicate, with 100 nm in thickness were deposited onto the bottom electrode with PECVD (Multichamber PECVD, STS-MULTIPLEX CLUSTER SYSTEM, England) at 300 °C (substrate temperature) and 200 W. The silicon nitride films, with a

thickness of 50 nm, were deposited with the same PECVD system using a  $\text{SiH}_4/\text{NH}_3/\text{N}_2$  mixture. The flow rates of  $\text{SiH}_4$ ,  $\text{NH}_3$  and  $\text{N}_2$  were fixed at 20, 80, and 510 sccm, respectively. Before the deposition of the top electrode, some samples were subjected to plasma treatment at 300 °C (substrate temperature). The  $\text{SiO}_2$  films were treated with  $\text{N}_2\text{O}$  plasma (with a flow rate of 200 sccm) for 30 min, while the  $\text{SiN}_x$  films were treated with  $\text{SiH}_4/\text{NH}_3$  plasma (the flow rate are 20 ( $\text{SiH}_4$ ) and 700 ( $\text{NH}_3$ ) sccm) for 30 min. Aluminum films (150 nm) were then deposited as the top electrodes.

Field emission scanning electron microscope (FE-SEM) (S-4700, Hitachi, Japan) was employed to observe the surface morphology and microstructure of the films. Atomic force microscope (AFM) (NS3a controller with D3100 stage, Veeco Instruments Inc., U.S.A.) was employed to measure the surface roughness. Auger electron microscope (AES) was employed to analyze elemental depth profiles. A C-V analyzer (model 590, Keithley Instruments Inc., U.S.A.) and a semiconductor parameter analyzer (HP4155B, Hewlett Packard Co., U.S.A.) were employed to measure the capacitance and the leakage current, respectively. The time to dielectric failure was defined when the current density exceeded  $0.5\text{A}/\text{cm}^2$ .

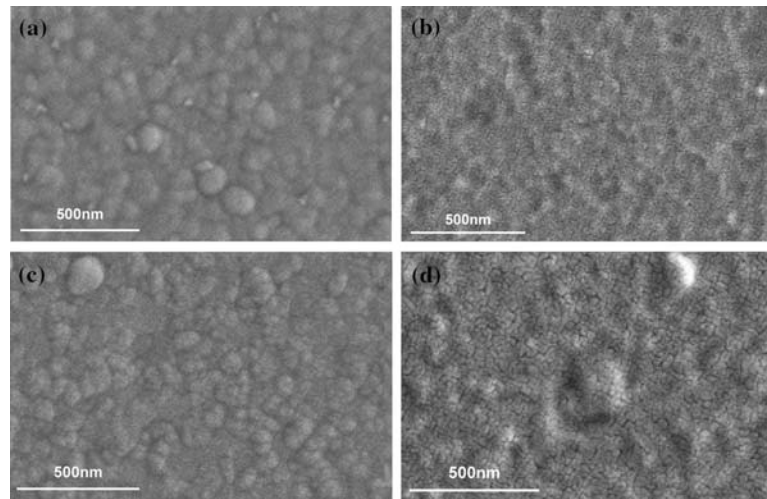
## Results and discussion

Figure 1 exhibits the surface morphologies of  $\text{SiO}_2$  and  $\text{SiN}_x$  films before and after plasma treatment. No apparent difference is observed between samples with and without plasma bombardment. However, plasma treatment increases the surface roughness of the oxide films while decreasing that of the nitride films. As shown in Fig. 2, the root-mean-square surface roughnesses are 0.541 and 0.579 nm for the as-deposited  $\text{SiO}_2$  and  $\text{SiN}_x$ , respectively, while those for the plasma-treated  $\text{SiO}_2$  and  $\text{SiN}_x$  films are 0.631 and 0.293 nm, respectively. The Auger depth profiles, exhibited in Fig. 3, suggest that there is no apparent difference between films with and without plasma treatment. However, the  $\text{SiN}_x/\text{Al}$  interface is more diffusive than the  $\text{SiO}_2/\text{Al}$  interface is.

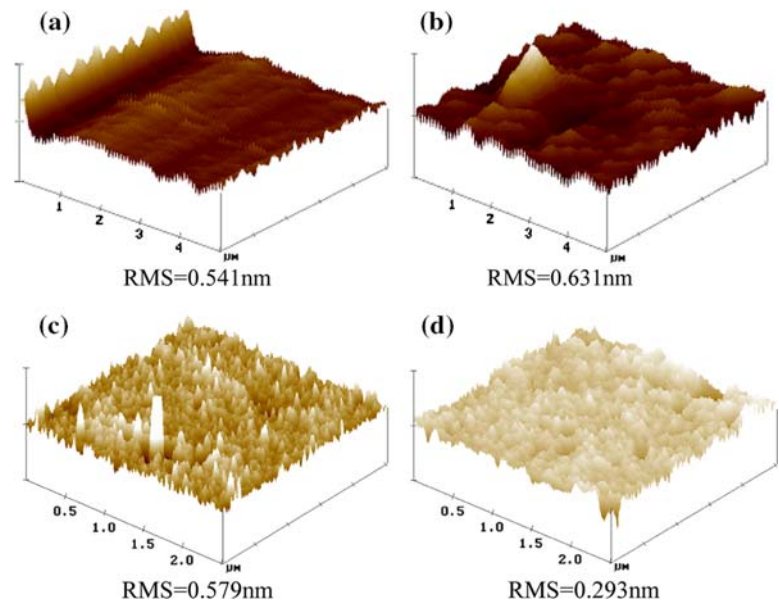
As summarized in Table 1, the capacitance densities increase from 1.02 to 1.21  $\text{fF}/\mu\text{m}^2$  for nitride capacitors and from 0.39 to 0.46  $\text{fF}/\mu\text{m}^2$  for oxide capacitors after plasma treatment. The voltage dependence of capacitance (C), as exhibited in Fig. 4, can be approximated by:

$$C = C_0(1 + AV + BV^2) \quad (1)$$

**Fig. 1** Surface morphologies of (a) as-deposited SiO<sub>2</sub>; (b) plasma-treated SiO<sub>2</sub>; (c) as-deposited SiN<sub>x</sub>; and (d) plasma-treated SiN<sub>x</sub>



**Fig. 2** AFM 3D images of surface morphologies and root-mean square (RMS) values of surface roughness of (a) as-deposited SiO<sub>2</sub>; (b) plasma-treated SiO<sub>2</sub>; (c) as-deposited SiN<sub>x</sub>; and (d) plasma-treated SiN<sub>x</sub>



where  $C_0$  is the capacitance at zero volt,  $A$  and  $B$  are the linear and quadratic coefficients of the capacitance, respectively. As shown in Table 1, for nitride capacitors, plasma treatment increases the absolute value of the linear coefficient from 22.1 to 91.5 ppm/V, while it decreases the absolute value of the quadratic coefficient from 27.9 to 9.8 ppm/V<sup>2</sup>. For oxide capacitors, the linear coefficients are 14.6 ppm/V (as-deposited) and 29.1 ppm/V (plasma-treated), and the quadratic coefficients are 13.4 ppm/V<sup>2</sup> (as-deposited) and 4.6 ppm/V<sup>2</sup> (plasma-treated). Also listed in Table 1 are the voltage coefficients of capacitance (VCC) from previous works for comparison [5, 7, 8]. The sensitivity of capacitance to bias voltage, i.e., VCC, is one of the important parameters for precision analog design. The specifications demanded by analog designers in the

VCC of high precision capacitors are  $A < 50$  ppm/V and  $B < 10$  ppm/V [5]. There are many factors which would affect the VCC of the capacitors, including: dielectric composition, processing conditions, dielectric thickness, frequency of measurement, voltage range of measurements and so on.

Plasma treatment eliminates the electrical hysteresis shift of the nitride capacitors. No hysteresis shift in the  $C$ - $V$  plot is observed for nitride capacitor with plasma treatment (Fig. 5a), while there is a 0.91 V shift for one without plasma treatment (Fig. 5b). For oxide capacitors, no hysteresis shift in the  $C$ - $V$  curve is observed. The hysteresis phenomenon is believed to be induced by the bulk silicon nitride traps such as: silicon dangling bonds near the nitride/electrode interface [6]. Fourier-transform infrared (FTIR) absorption spectra of the

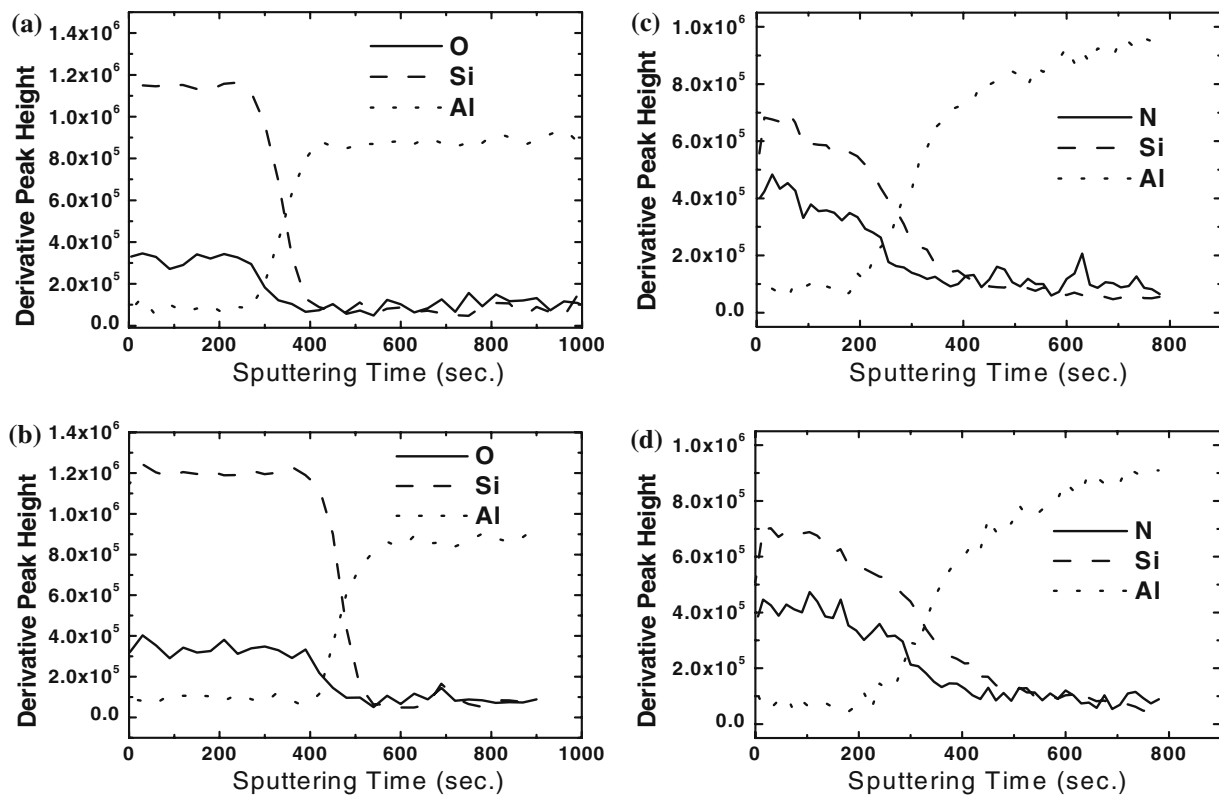


**Fig. 3** Auger depth profiles of (a) as-deposited SiO<sub>2</sub>; (b) plasma-treated SiO<sub>2</sub>; (c) as-deposited SiN<sub>x</sub>; and (d) plasma-treated SiN<sub>x</sub>

**Table 1** Capacitance density and voltage coefficient of capacitance,  $A$  and  $B^*$ , of several nitride and oxide MIM capacitors at 100 kHz

Capacitance density (fF/ $\mu\text{m}^2$ )	Voltage range of measurement	Dielectric thickness (nm)	$A$ (ppm/V)	$B$ (ppm/V <sup>2</sup> )	Note
1.02 (as-deposited nitride)	10V to -10V	50	-22.1	27.9	This work
1.21 (plasma-treated nitride)	10V to -10V	50	91.5	-9.8	
0.39 (as-deposited oxide)	10V to -10V	100	-14.6	-13.4	This work
0.46 (plasma-treated oxide)	10V to -10V	100	29.1	-4.6	
1.1 (nitride)	5V to -5V	60	25.5	9.3	Ref. 1
1.2–1.35 (nitride)	5V to -5V	50	-21 to -14	5.5–8	Ref. 7
2.0 (nitride)	6V to -6V	30	-153	62.3	Ref. 8

\* $C = C_0(1 + AV + BV^2)$ .  $C_0$  and  $C$  are the capacitances at 0 and  $V$  volts, respectively

SiN<sub>x</sub> films suggested an increase in absorption of Si–H bond after SiH<sub>4</sub>/NH<sub>3</sub> plasma treatment. As indicated in Fig. 6, the ratio of Si–H peak ( $\sim 2,160\text{ cm}^{-1}$ ) to Si–N peak ( $\sim 890\text{ cm}^{-1}$ ) increases from 9% of the as-deposited SiN<sub>x</sub> films to about 16–19% of the plasma treated ones. Previous work by Huylenbroeck et al. suggests that formation of silicon–hydrogen bonds after plasma bombardment reduces the number of traps presents in the SiN<sub>x</sub> films [5]. Auger depth profile results indicate a slight increase of nitrogen to silicon ratio of the SiN<sub>x</sub> films after plasma treatment. It is argued that SiH<sub>4</sub>/NH<sub>3</sub> plasma bombardment raised the nitrogen to silicon ratio and/or formed the Si–H bond at the interface region. These are two of the possible reasons

why electrical hysteresis shift is not observed for SiH<sub>4</sub>/NH<sub>3</sub> plasma treated SiN<sub>x</sub> films.

The current density ( $J$ ) versus electrical field ( $E$ ) curves, shown in Fig. 7, indicates a decrease of the leakage current density after plasma treatment. The leakage current of the oxide capacitors drops from  $1.90 \times 10^{-7}\text{ A/cm}^2$  of the as-deposited films to  $2.91 \times 10^{-10}\text{ A/cm}^2$  of the plasma-treated ones at 1.0 MV/cm. It is argued that the incorporation of nitrogen into the oxide films after N<sub>2</sub>O plasma treatment reduces strained Si–O bonds and silicon dangling bonds, thus, consequently, reduces interface defects and improves the  $J$ – $E$  characteristics of the SiO<sub>2</sub> films [9]. The leakage current of the nitride

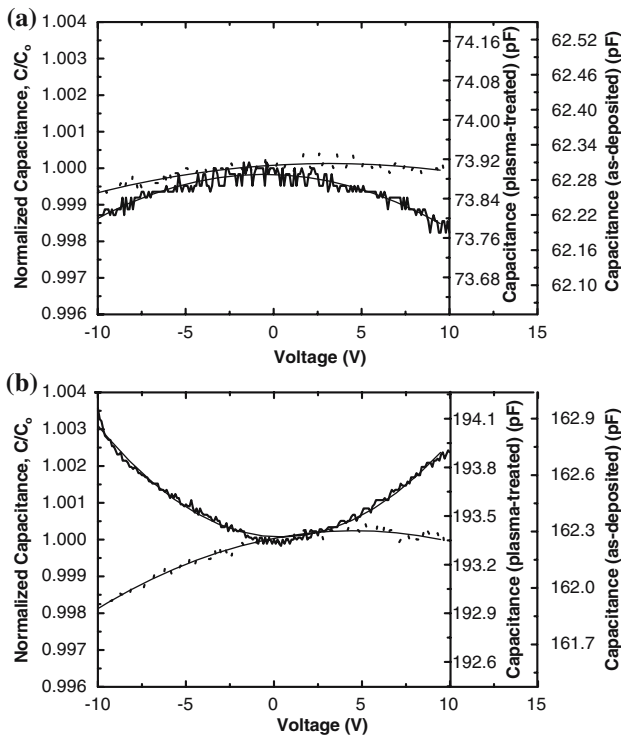


**Fig. 4** Capacitance ( $C$ ) as a function of the dc voltage of (a) oxide and (b) nitride MIM capacitors with (▲) and without (□) plasma treatment. The curves exhibit quadratic behavior in the voltage coefficient of capacitance (VCC).  $C_0$  is the capacitance value measured at zero volt

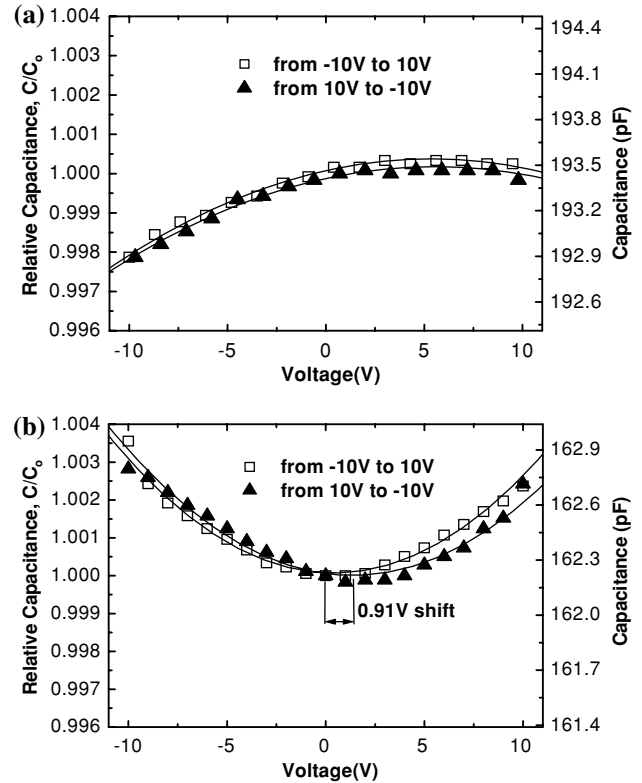


**Fig. 5** Capacitance ( $C$ ) as a function of the dc voltage of nitride MIM capacitors (a) with and (b) without plasma treatment.  $C_0$  is the capacitance value measured at zero volt

capacitors at 1.0 MV/cm reduces from  $1.79 \times 10^{-9} \text{A/cm}^2$  (as-deposited) to  $8.99 \times 10^{-10} \text{A/cm}^2$  (plasma-treated). Both the band gap and the barrier heights at the metal–insulator interfaces of the nitride films increase with the increase of the N content [10]. As mentioned previously, the nitrogen concentration increases after plasma treatment. Hence, the decrease of the leakage current is attributed to the reduction of the trap densities, the raise of the energy band gap and/or the increase of the barrier height. Figure 8 exhibits the time ( $t$ ) dependence of the current density ( $J$ ) of nitride capacitors at various stress fields. The  $J$ – $t$  curves of specimens without plasma treatment show an initial increase of the current density with time followed by a decrease of  $J$  with  $t$  before the breakdown of the dielectric, while the current density of the plasma-treated samples increases slightly before the breakdown of the dielectric. Besides, although the current density of the plasma-treated capacitors is smaller, the time to dielectric breakdown (TTDB) is shorter. Van Delden and van der Wel proposed a degradation mechanism for PECVD silicon nitride films [10]. According to the proposed model, the electron-hole recombination breaks the

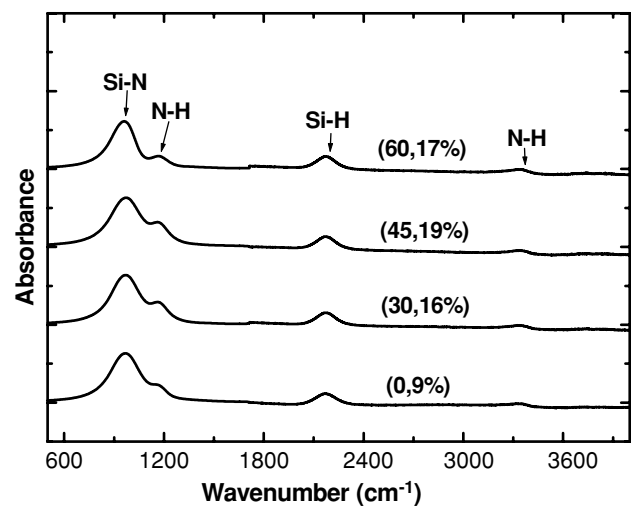


**Fig. 6** The FTIR absorbance spectra of silicon nitride films as a function of plasma treatment time. Data in the parenthesis ( $t$ ,  $R$ ) are the plasma treatment time in minutes and the peak ratio of Si–H ( $2,160 \text{cm}^{-1}$ ) to Si–N ( $\sim 890 \text{cm}^{-1}$ )

weaker Si–Si and Si–H bonds to form the Si dangling bonds which are singly occupied for the neutral state ( $\text{Si}_3^0$ ). These neutral states trap charge carriers of

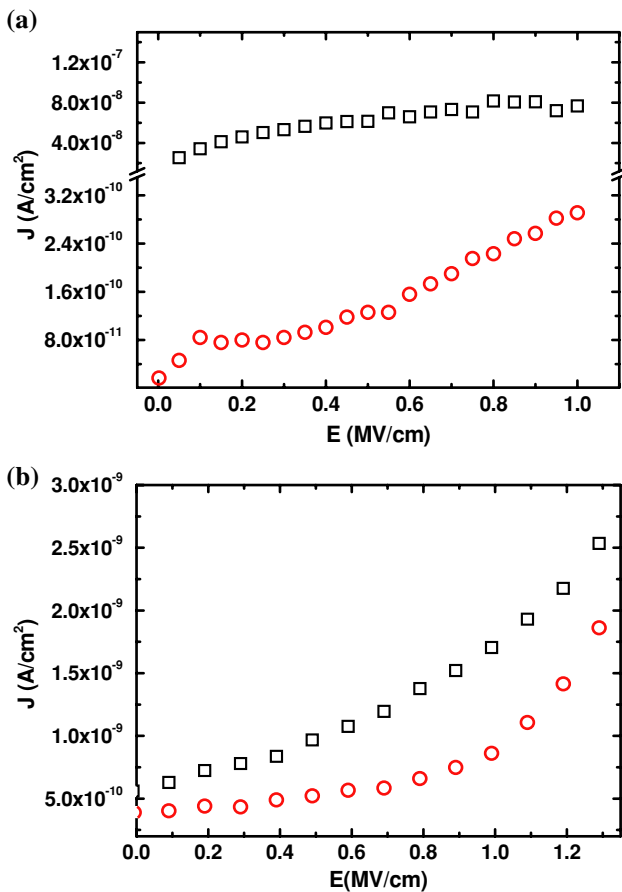


**Fig. 7** Current density ( $J$ ) versus electrical field ( $E$ ) of as-deposited ( $\square$ ) and plasma-treated ( $\circ$ ) (a)  $\text{SiO}_2$  and (b)  $\text{SiN}_x$  MIM capacitors measured at room temperature

either sign to form  $\text{Si}_3^+$  and  $\text{Si}_3^-$  centers. The  $\text{Si}_3^+$  center may react with N–H to form Si–N and leave a net concentration of negatively charged  $\text{Si}_3^-$  centers. For

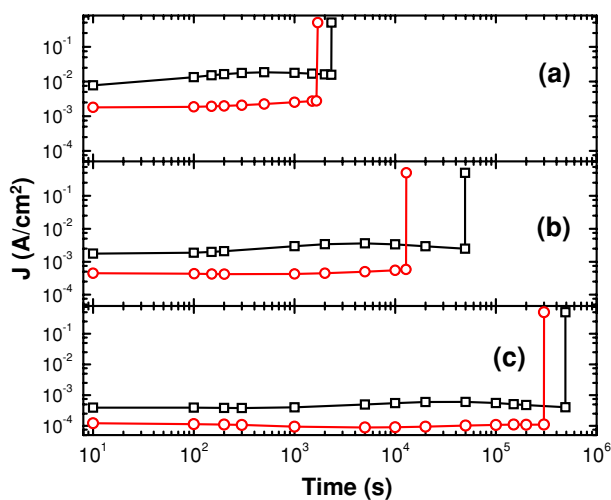


**Fig. 8** Time dependence of the current density of nitride capacitors with ( $\circ$ ) and without ( $\square$ ) plasma treatment at (a) 6.0 MV/cm; (b) 5.5 MV/cm; and (c) 5.0 MV/cm

samples without plasma treatment, the initial increase of  $J$  with time ( $t$ ) is due to an increase of defects in the band edges. Then, silicon dangling bonds which are occupied for the neutral states ( $\text{Si}_3^0$ ) trap electrons and thus reduce the total current, as shown in Fig. 8. On the other hand, the  $\text{SiH}_4/\text{NH}_3$  plasma raised the nitrogen to silicon ratio and/or formed the Si–H bond at the interface region as discussed previously. The number of the silicon dangling bond is decreased after plasma bombardment. Hence, the current density is smaller and increases slightly before breakdown. Besides, the plasma-treated samples have higher concentration of the weaker Si–H bonds which lead to the shorter lifetime ( $t_F$ ). Figure 9 exhibits the  $t_F$  as a function of stress field. The field-acceleration parameter  $\gamma$  is, defined as [11]:

$$\gamma = - \left[ \frac{\partial \ln(t_F)}{\partial E} \right] \tag{2}$$

Since  $\gamma$  denotes the field dependence of the lifetime, capacitors with smaller  $\gamma$  (i.e. those with plasma treatment) have to be operated at voltages much lower than its breakdown voltage as compared to those with larger  $\gamma$  (i.e. without plasma treatment) [11]. The field-acceleration parameters ( $\gamma$ ) of the as-deposited and plasma-treated nitride films are 6.13 and 6.05, respectively. The difference in the  $\gamma$  value is small, hence, the effect of plasma treatment on the field-acceleration parameter is not appreciable.

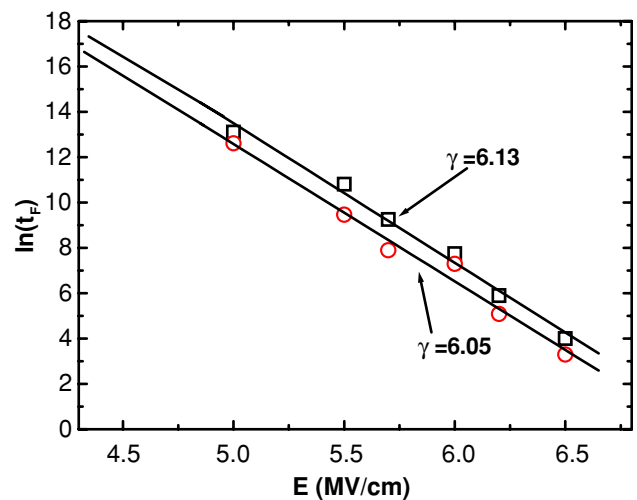


**Fig. 9** Failure time ( $t_F$ ) versus electrical field ( $E$ ) of nitride capacitors with ( $\circ$ ) and without ( $\square$ ) plasma treatment. The field-acceleration parameter ( $\gamma$ ) is defined as  $\gamma = - \left[ \frac{\partial \ln(t_F)}{\partial E} \right]$

## Conclusions

In this study,  $\text{SiH}_4/\text{NH}_3$  and  $\text{N}_2\text{O}$  plasmas are used to bombard nitride and oxide films of MIM capacitors, respectively. No apparent difference in the surface morphology of both the  $\text{SiO}_2$  and  $\text{SiN}_x$  films is observed between samples with and without plasma bombardment. The  $\text{SiH}_4/\text{NH}_3$  plasma treatment eliminates the electrical hysteresis shift of the nitride MIM capacitors. The FTIR spectra reveal an increase of Si–H bonds after plasma treatment and suggest that hydrogen atoms were introduced into the  $\text{SiN}_x$  films to form silicon–hydrogen bonds which reduced the number of traps present in the  $\text{SiN}_x$  films, and, consequently, eliminated the electrical hysteresis shift. The leakage current density of both the oxide and nitride capacitors decrease after plasma treatment. For oxide capacitors, the incorporation of nitrogen into oxide films reduces interface defects and, hence, the leakage current. For nitride capacitors, there are several possibilities for the decreased leakage current after plasma treatment, such as: the reduction of the trap densities, the raise of the energy band gap and/or the increase of the barrier height. No appreciable difference in the field-acceleration parameter is observed between specimens with and without plasma treatment.

**Acknowledgements** This work is sponsored by National Science Council, Taiwan, under the contract number NSC 93-2216-E-009-023.

## References

1. Chang TY, Chen HW, Lei TF, Chao TS (2002) *IEEE Trans Electron Devices* 29:2163
2. Chang TY, Lei TF, Chao TS, Wen HC, Chen HW (2002) *IEEE Electron Device Lett* 23:389
3. Lim BC, Choi YJ, Choi JH, Jang J (2000) *IEEE Trans Electron Devices* 47:367
4. Chen CT, Chiou BS (2004) *J Mater Sci Mater Electron* 15:139
5. Van Huylbroeck S, Decoutere S, Venegas R, Jenei S, Winderickx G (2002) *IEEE Electron Device Lett* 23:191
6. Lau WS (1990) *Jpn J Appl Phys* 29:L690
7. Kar-Roy A, Hu C, Racanelli M, Compton CA, Kempf P, Jolly G, Sherman PN, Zheng J, Zhang Z, Yin A (1999) in *Proceedings of the 2nd IEEE International Interconnect Technology Conference*, San Francisco, USA, May 1999 (IEEE, New York, USA) p 245
8. Babcock JA, Balster SG, Pinto A, Dirnecker C, Steinmann P, Jumpertz R, El-Kareh B, (2001) *IEEE Electron Device Lett* 22:230
9. Kaluri SR, Hess DW (1998) *J Electromchem Soc* 145:662
10. Van Delden MHW, Van Der Wel PJ (2003) in *Proceedings of the 41st International Reliability Physics Symp.* Dallas, USA, March 2003 (IEEE, New York, USA) p. 293
11. Mcpherson JW, Kim J, Shanware A, Mogul H, Rodriguez J (2003) *IEEE Trans Electron Device* 50:1771